Design and test of VSC assisted resonant current (VARC) DC circuit breaker

L Ängquist, S Nee*, T Modeer*, A Baudoin*, S Norrga*, N A Belda †*

**SCiBreak AB, Sweden,* *†DNV GL KEMA Laboratories, The Netherlands*
**lennart@scibreak.com* *†Nadew.Belda@dnvgl.com*

Keywords: Circuit-breaker, HVDC

Abstract

This paper presents the VSC assisted resonant current (VARC) direct current circuit-breaker concept, which comprises a vacuum interrupter, operated by an ultra-fast actuator, together with a power electronic converter that creates a zero-crossing in the arc current. A few main circuit topologies are shown and discussed and a dynamic model of the DC link voltage in the VSC is presented. A module rated for 10 kA against 40 kV transient interruption voltage has been built and tested at an independent test laboratory, and some test results are presented.

1 Introduction

Cost-effective, fast-acting (within few milliseconds) direct current circuit-breakers (DCCB) have been on the wish-list for HVDC developers and other users of DC technology at voltages above a few kilovolts for a long time [1]. Driven by the ever-increasing power handling capability of semiconductor devices, several concepts using mechanical current-interrupters assisted by power electronic auxiliary circuits have been developed and tested. Most often the mechanical interrupter is a vacuum interrupter (VI).

One such concept is the "VSC assisted resonant current" (VARC) DCCB, which utilizes a voltage source converter (VSC), having low output voltage, to excite an oscillating current passing through the VI and a parallel resonant branch [2]. The required oscillating current peak level is reached within less time than the time needed to separate the contacts in the VI.

The aim of this paper is to give some insight in the design of the oscillating current excitation system, to discuss possible circuit topologies, to describe the exchange of energy between the resonant link and the DC link in the exciting converter, and finally to present some results obtained in laboratory testing.

2 DCCB concepts based on oscillating current

Mechanical circuit-breakers (CB) can successfully interrupt current upon separation of its contacts if and only if the current, naturally or artificially, is brought to an instantaneous zero. Alternating current (AC) with rated frequency 50/60 Hz provides such zero crossings naturally with 100/120 Hz frequency. Direct current (DC), on the other hand, does not experience any zero-crossings at all, and CBs interrupting such current need to create current zeros by artificial means.

The arc in certain types of CBs, e.g. SF6-breakers, exhibits a negative differential resistance when the contacts separate, and the so-called "passive resonant DCCBs" have been designed exploiting this property to excite an oscillating current in a resonant circuit connected in parallel with the contact terminals, see figure 1a. The amplitude of the oscillating current grows until zero-crossings occur in the arc current and interruption happens as shown in figure 1b. However, the operation time becomes long, several tens of milliseconds, due to the limited value of the negative resistance, making this solution type of circuit-breaker too slow to be used in meshed HVDC networks for fault clearing applications.

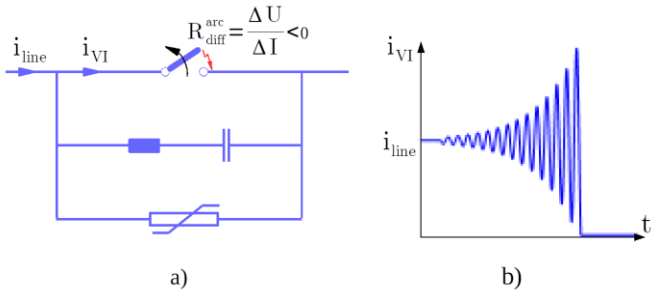

Figure 1: Passive resonant DCCB

In the VARC DCCB concept the oscillating current is excited by a power electronic VSC, which is controlled with positive feedback, so that the output voltage is synchronized with the converter current. Any desired amplitude growth can be achieved by design and the excitation becomes independent of the characteristics of the arc between the contacts. A VI could therefore be utilized.

DCCBs for high voltages, up to 320 or 500 kV, can be designed from several modules connected in series as shown in figure 2. A residual breaker is connected in series, as shown in the figure, to provide full isolation after current interruption by the DCCB.

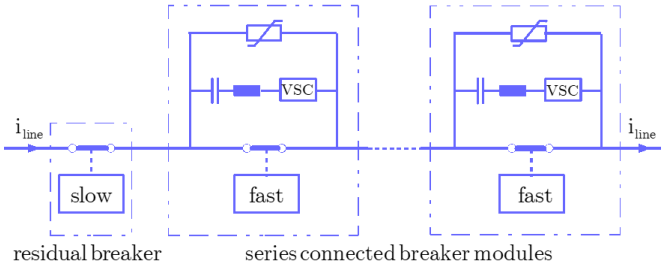

Figure 2: HVDC CB constituted of series-connected modules

3 Current excitation principles

The basic formulas for the amplitude of the excited current can be derived from the simple circuit shown in figure 3.

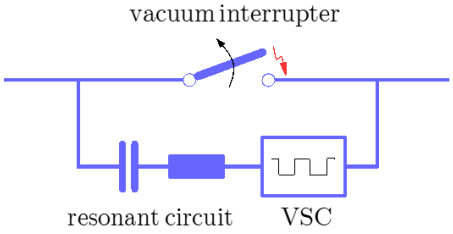

a)

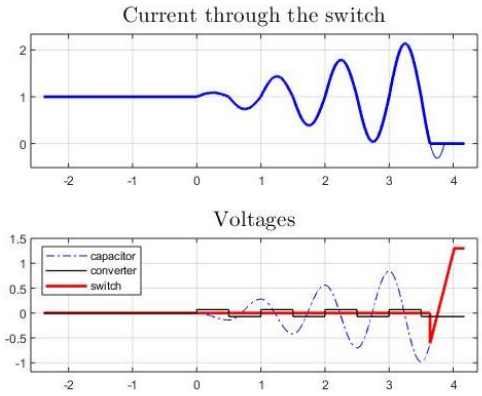

b)

Figure 3: Resonant circuit with VSC

When the contacts separate the line current flows through an arc between the mechanical contacts in a VI. A branch comprising a resonant circuit and a series-connected VSC is connected in parallel with the interrupter terminals. The resonant circuit has characteristic impedance and resonant frequency

$$Z_{LC} = \sqrt{\frac{L}{C}} \qquad f_{LC} = \frac{1}{2\pi\sqrt{LC}} \tag{1}$$

and the voltage in the VSC DC link is U_{DC}.

The VSC output voltage is zero until it is enabled at $t = 0$. A first voltage step, U_{DC}, is applied to the resonant circuit resulting in a current pulse with amplitude $I_0 = \frac{U_{DC}}{Z_{LC}}$ (losses are neglected) peaking at $t_n = ½\pi\sqrt{LC}$. A half-cycle later the VSC excutes a reversal applying a voltage step $-2U_{DC}$ on the resonant circuit, adding current amplitude $2I_0$, making the new amplitude $3I_0$. Similarly after *n* reversals the amplitude of the oscillating current becomes

$$I_n = (2n+1)I_0 \tag{2}$$

and the peak current after *n* reversals appears at time

$$t_n = (n+½)\pi\sqrt{LC} \tag{3}$$

4 VARC main circuit design aspects

The resonant frequency is selected such that the necessary number of reversals can be executed in the time from trip command until the end of current neutralization. The required DC link voltage reduces with increasing number of reversals and hence the total voltage rating of the VSC semiconductors can be decreased. However, losses and DC voltage drop in the VSC put a limit to the number of achievable useful reversals.

The metal oxide varistors (MOV) shown in figure 2 play a very important role in the design of each module of the DCCB. They limit the counter-voltage generated by each module at current interruption, thereby protecting both the network components and the current-interrupting VI in the CB against too high voltage stress. In doing so they absorb magnetic energy stored in the system inductance [3]. On the other hand, the protective level of the MOV voltage must not be too low as it must significantly exceed the highest operational voltage of the connected network. Too low protective voltage causes long time to quench the line current and very large energy absorption in the MOV. Typically, the protective voltage level in the MOV is selected to be 1.5 times the rated system voltage.

The main circuit in a VARC DCCB module could be configured in various ways, as shown in figures 4 a)-c). The difference between these configurations is mainly the connection of MOV to the rest of the circuit.

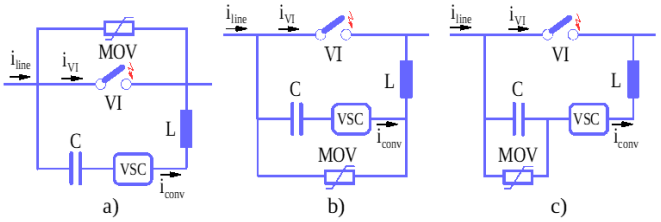

Figure 4: Different main circuit configurations

During the current excitation phase, i.e. while the MOV is not conducting, these configurations behave identically. The basic waveforms for current and voltage are shown in the diagrams in figure 3. The diagram in figure 3a shows the superposition of the line current and the oscillating current, constituting the current through the VI. The current zero occurs when the amplitude of the oscillating current reaches the line current amplitude and the VI interrupts.

The diagram in figure 3b shows the capacitor voltage. It is a sinusoidally oscillating curve with increasing amplitude until current-zero through the arcing VI is achieved. Then the arc in the current interrupter is extinguished and the line current commutates to the parallel resonant circuit. The inductive voltage drop in the resonant circuit inductor can be neglected as the line current has a much lower time derivative than the oscillating current. The capacitor voltage increases almost linearly until the total voltage across the VSC and the resonant capacitor reaches the protection level of the MOV and the current commutates into the latter.

It should be noted that the inductor in the resonant circuit carries the entire line current at the instant when the current starts to commutate into the MOV. The current commutation from an inductor does not happen instantaneously. Therefore, in the configuration shown in figure 4a the line current continues to charge the capacitor to a voltage that considerably exceeds the protection level of the MOV before the line current fully commutates into the MOV. This property makes it difficult to propose a safe design for this configuration, and accordingly it is abandoned.

In the configurations shown in figures 4b-4c, on the other hand, the voltage across the series-connection of the capacitor and the VSC (figure 4b), or across the capacitor only (figure 4c), is strictly limited by the MOV as very low stray inductance between the capacitor and MOV branches permits current to commutate almost instantaneously between these branches.

The two topologies in figures 4b-4c differ with respect to the duration of current flow through the VSC. In the configuration shown in figure 4b the VSC is conducting until the protective voltage of the MOV is reached. In the configuration shown in figure 4c the VSC conducts the line current until it is brought to zero (leakage level) by the MOV. The duration of this conduction interval depends on the inductance in the connected network, the difference between the MOV protective voltage and the system voltage in the connected network and the magnitude of line current being interrupted [3][4]. The VSC conduction times may differ considerably from a fraction of a millisecond for the configuration in figure 4b to tens of milliseconds for the one in figure 4c.

The design of the main circuit is based on the desired current interrupting capability I_{BRK} and the maximum voltage U_{MOV} produced by the MOV during interruption. U_{MOV} must exceed the maximum system voltage of the connected network to be able to neutralize the current growth and to suppress the line current. Typically, U_{MOV} is 1.5 times system voltage in the connected network. The quotient between U_{MOV} and I_{BRK} defines an impedance $Z_{BRK} = \frac{U_{MOV}}{I_{BRK}}$.

In the configurations in figures 4b-4c it must be possible to excite an oscillating current with an amplitude that exceeds the maximum current to be interrupted, I_{BRK}. Meanwhile, the corresponding capacitor voltage must not reach the MOV voltage level, U_{MOV}. Accordingly

$$Z_{LC} I_{BRK} < U_{MOV} = Z_{BRK} I_{BRK} \tag{4}$$

and the impedance Z_{BRK} must fulfil the condition

$$Z_{LC} < Z_{BRK} . \tag{5}$$

Another important fact is that reignitions may occur across the VI contacts at or immediately after current interruption. In this case a high voltage step appears across the resonant circuit and it will be accompanied by a correspondingly high current pulse that is essentially limited only by Z_{LC}. Therefore, it is desirable to make Z_{LC} as high as possible to keep the current pulse amplitude at reignition as low as possible.

To conclude: it is desirable to make the main circuit impedance Z_{LC} lower than, but close to, Z_{BRK}. The amplitude of the current pulse at reignition then becomes just a little higher than the normal maximum peak current I_{BRK}.

5 Interaction between the resonant circuit and the DC link

Energy is transferred from the DC link in the VSC to the resonant circuit during excitation of the oscillating current. The DC link voltage therefore decreases from its initial value during the excitation process. Enough capacitance, C_{DC}, must be provided to ensure that the desired current oscillation amplitude can be achieved.

In a simple model the details of the oscillating current can be disregarded and only the growth of its envelope, $\hat{i}_{LC}(t)$, then is being considered. The dynamics of the oscillating current amplitude is determined by the sum of an exciting term $\frac{d\hat{i}_{DC}^{grow}}{dt}$ and a term representing the losses in the resonant circuit $\frac{d\hat{i}_{DC}^{loss}}{dt}$. The current amplitude is increased by $\frac{2u_{DC}}{Z_{LC}}$ per reversal of the converter, thus

$$\frac{d\hat{i}_{LC}}{dn} = \frac{2u_{DC}}{Z_{LC}} . \tag{6}$$

The number of reversals at oscillation frequency f are $n = 2t\,f$ and the behaviour of the growth term of the current envelope then becomes

$$\frac{d\hat{i}_{LC}^{grow}}{dt} = \frac{d\hat{i}_{LC}^{grow}}{dn}\frac{dn}{dt} = \frac{2u_{DC}}{Z_{LC}} 2f = \frac{4fu_{DC}}{Z_{LC}} . \tag{7}$$

This expression describes the envelope growth if no losses are considered. The losses can be described by the quality factor Q_{LC} for the resonant circuit, which could be interpreted as a

resistance $R = \frac{Z_{LC}}{Q_{LC}}$ inserted in series with the resonant circuit. The current amplitude then decays with the exponential factor $e^{-\frac{\omega t}{2Q_{LC}}} = e^{-\frac{\pi ft}{Q_{LC}}}$ causing the 'already' excited current envelope to decline by a rate determined by Q_{LC} as

$$\frac{d\hat{i}_{LC}^{loss}}{dt} = -\frac{\pi f}{Q_{LC}}\hat{i}_{LC}. \quad (8)$$

The total rate of change of the envelope of the current is the sum of the exciting and the loss terms

$$\frac{d\hat{i}_{LC}}{dt} = \frac{4fu_{DC}}{Z_{LC}} - \frac{\pi f}{Q_{LC}}\hat{i}_{LC}. \quad (9)$$

The rate of change of the voltage over the DC-link is accounted for by the loss of charge to the resonant current. Since the current envelope is considered, and the waveform of the actual current through the DC-link is of the form $\hat{i}_{LC}\left|\sin(\omega t)\right|$, an adapting factor $\frac{2}{\pi}$ is used to relate the envelope current to the discharge current from the DC-link capacitor

$$C_{DC}\frac{du_{DC}}{dt} = -\frac{2}{\pi}\hat{i}_{LC}. \quad (10)$$

The above model was integrated in an example to illustrate the impact of losses in the resonant circuit.

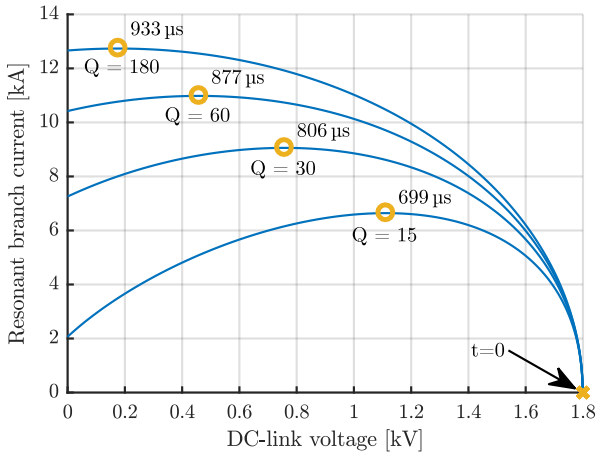

Figure 5: Mathematical model trajectories for u_{DC} vs $\hat{i}_{LC}$ for varying $Q_{LC} = 15, 30, 60, 180$, $C_{DC} = 3$ mF, $Z_{LC} = 3.2\ \Omega$ at $f = 10$ kHz.

In figure 5 curves for different values of Q_{LC} at $f = 10$ kHz are shown. The circles denote the maximum achievable resonant current envelope for each value of Q_{LC}. Note that the maximum achievable current is reduced by 50% when the quality factor drops from $Q_{LC} = 180$ to $Q_{LC} = 15$ at frequency $f = 10$ kHz. It can be concluded that the losses in the resonant circuit, particularly in the inductor, play an important role.

The energy in the resonant circuit is $W_{LC} = ½LI_{BRK}^2$ when the oscillating current amplitude is I_{BRK}. The initial energy in the DC link capacitor of the VSC, $W_{DC0} = ½C_{DC}u_{DC0}^2$, must exceed this value to enable excitation of the oscillating current to the desired level. Higher initial energy available in the DC link of the VSC makes the excitation time shorter, as the voltage drop in the DC link becomes smaller. An example is shown in the diagram in figure 6a. The parameters in this example are $I_{BRK} = 10$ kA, $C_{DC} = 3$ mF, $Z_{LC} = 3.2\ \Omega$, $f = 10$ kHz and $Q_{LC} = 120$. The diagram shows that, for the actual quality factor, the initial energy in the DC link must exceed the final energy W_{LC} by at least 25%.

The diagram in figure 6b shows the fraction of the initial DC link energy that is used during excitation to amplitude I_{BRK}. The information in the two diagrams in figure 6 can be used to estimate the required DC link energy in an OPEN-CLOSE-OPEN sequence without intermediate charging. If the initial energy in the DC-link is $2.5 \times W_{LC}$, then 56%, i.e. $1.4 \times W_{LC}$, remains after the first OPEN operation according to the diagram in figure 6b. The diagram in figure 6a shows that, with the remaining energy $1.4 \times W_{LC}$, the second OPEN operation can still be executed with some margin.

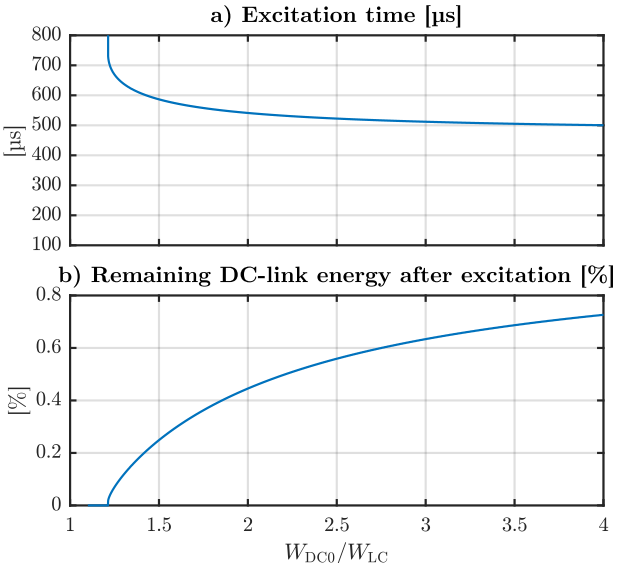

Figure 6: Example showing impact of relative initial DC link energy W_{DC0}/W_{LC} in the VSC: a) excitation time to 10 kA, b) remaining DC link energy after excitation to 10 kA.

6 Experimental results

A module prototype adapted to interrupt 10 kA peak against transient interruption voltage (TIV) 40 kV peak has been designed and built. A photo of the module is shown in figure 7. Its mechanical design allows vertical stacking of several modules on top of each other. The external dimensions of the module were 2.2×1.7×1.6 m^3 and the total mass was 800 kg.

The module was equipped with a 160 kg MOV package with a total energy absorption capability of 2 MJ.

Figure 7: Prototype of module for VARC DCCB

The TIV is determined by the protective voltage of the 12MOV. The module comprises a VI rated for 24 kV 1250 A equipped with a prototype ultra-fast actuator using the Thomson coil principle. At opening operation a contact gap of 6 mm was obtained 3 ms after trip command. A second VI, rated 24 kV 800 A, operated by a standard permanent-magnet type actuator, was included and used as a residual breaker (see figure 2). The converter had two series-connected single-phase, full-bridge VSCs equipped with standard IGBT modules. The module was equipped with necessary sensors, gate drivers, chargers for DC links etc.

The module was tested at DNV GL KEMA High-power Laboratory in Arnhem, the Netherlands, in June 2018. A photo of the test setup is shown in figure 8. The test circuit was designed based on AC short-circuit generator(s) running at 16.7 Hz, which allowed tests with short-circuit currents having different characteristics. The value and rate-of-rise of the short-circuit current at the trip instant as well as the total amount of energy to be absorbed by the MOV package could be varied within wide ranges.

Several tests to demonstrate different current (magnitude) interruption capabilities of the module were performed at 5 kA, 8 kA and 10 kA. A recording from one such test is reproduced in figure 9, where the complete current interruption process at 10 kA can be seen.

Figure 8: Photo of the VARC module tested at DNV GL KEMA Laboratories, Arnhem, the Netherlands

During the test procedure the short-circuit current rises and passes the trip level at time *t=0*. Contact separation 6 mm is achieved 3 ms later, and at this time the oscillating current has reached the level of the applied short-circuit current. The oscillating current is excited while the contacts approach the desired contact gap and the current zero-crossing is achieved when sufficient contact gap has been reached, approximately 3 ms after the trip command was given. The current in the VI is interrupted and the line current commutates into the MOV, which sets up a voltage of 40 kV, which in turn exceeds the driving voltage in the generator and causes the line current to decrease and to finally disappear after another 3 ms.

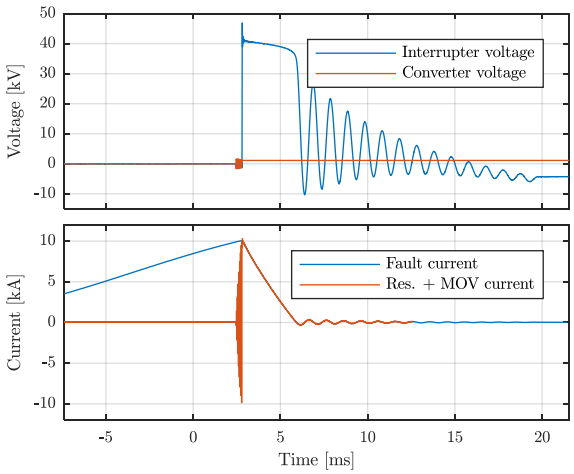

Figure 9: Current interruption at 10 kA with TIV 40 kV

In figure 10 the same recording is shown with higher resolution in another time scale. It shows that excitation of the oscillating current is performed in this case by fifteen reversals. The amplitude of the VSC output voltage the should be approximately $40/(2\times15+1)=1.3\,\text{kV}$ according to the simple ideal model used to derive equation (2). The real initial DC link voltage in the test was 1.5 kV. The deviation is caused

by the very idealized model that does not take losses or voltage drop in the VSC DC-links into account.

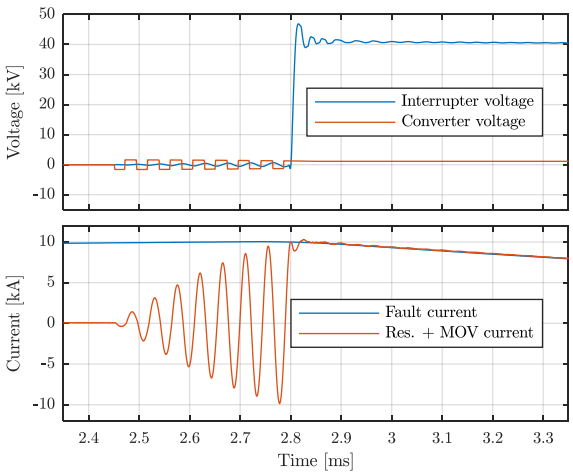

Figure 10: Details from figure 9 close to current interruption.

Another interesting property of the VARC concept is demonstrated in figure 11, where the recordings of interruption of short-circuit currents with different amplitudes are compared.

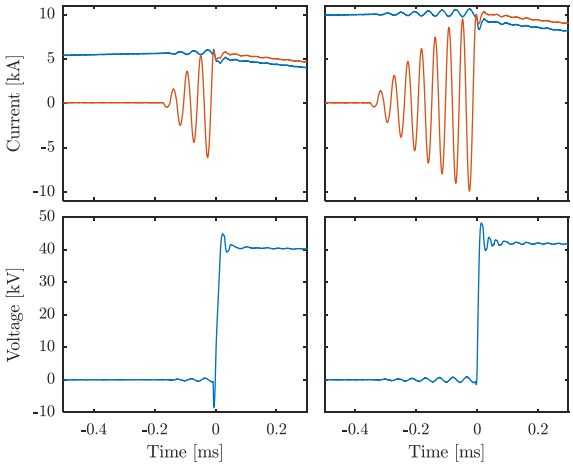

Figure 11: Comparison of interruptions at 5 kA and 10 kA.

The upper diagrams show the line current and the sum of the oscillating current and the current through the MOV. The contribution from the MOV current can be neglected before the interruption, and accordingly the interruption occurs when the oscillating current equals the line current. The diagrams illustrate that the amplitude of the pulse that causes current zero-crossing is adapted to the level of the short-circuit current to be interrupted.

The VARC DC CB is bidirectional by nature. This feature is also demonstrated in figure 12, where currents with opposite directions are being interrupted by the tested module. References for the control system remain unchanged in the two tests.

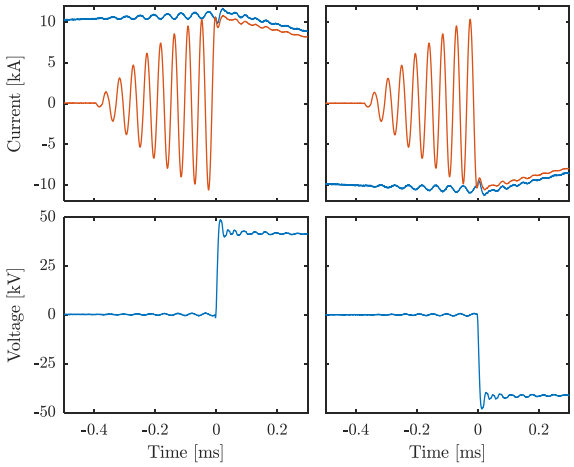

Figure 12: Interruption with opposite current directions.

7 Conclusions

The VARC concept for a DC CB is described in this paper. Various main circuit configurations and design of its main components have been discussed. A model of the dynamics of the energy exchange between the VSC DC link and the resonant circuit has been presented. Some experimental results from testing of a prototype module rated for interruption of 10 kA against a TIV of 40 kV also have been presented.

Acknowledgements

The work described in this paper was made possible thanks to the support of InnoEnergy Scandinavia, Svenska Kraftnät, and the Swedish Energy Agency. This work was supported by the European Union's Horizon 2020 research and innovation program under grant No. 691714.

References

[1] CIGRE WG B4:52: Feasibility of HVDC grids, *CIGRE Technical brochure 533*, Paris, April 2013.
[2] L. Ängquist, S. Norrga, T. Modeer, S. Nee, "Fast HVDC breaker using reduced-rating power electronics,"*ACDC 2017, paper 70*, Manchester, GB, February 2017.
[3] N. A. Belda and R. P. P. Smeets, "Test Circuits for HVDC Circuit Breakers," *IEEE Transactions on Power Delivery*, vol. 32, no. 1, pp. 285-293, 2017
[4] N. A. Belda, C. Plet and R. P. P. Smeets, "Analysis of Faults in Multi Terminal HVDC Grid for Definition of Test Requirements of HVDC Circuit Breakers," *IEEE Transactions on Power Delivery*, vol. 33, no. 1, pp. 403-411, 2018.